Section 2
ADVANCED TECHNOLOGY DEVELOPMENTS

2.A The Study of Shock Launching in Silicon Using Pulsed X-Ray Diffraction

The laser generation of shocks encompasses a wide range of physical processes and effects, since virtually every property of condensed matter can be altered with pressure. Particular areas of scientific study in which laser-generated shocks may find application include energetic materials,[1] high-velocity impacts,[2] and the alteration of the materials properties of certain alloys and ceramics.[3] For the more conventional shock drivers, the shock-launching region – i.e., the initial layer of the material of interest from which the shock begins – is obscured by the driving mechanism. Also, the timing of diagnostic apparatus is not readily accomplished on the subnanosecond time scale necessary to directly observe the launching of a shock wave into a lattice. For this reason, well-resolved experimental studies of the shock-launching region up to now have been intractable. Laser-driven shocks do not present this limitation.

We report results of an experiment in which we probed the initial few (4 to 5) microns of the shock-launching region in silicon with pulsed x rays, and directly measured the temporal variation of lattice spacing by Bragg x-ray diffractometry. We have also examined the experimentally determined peak density as a function of laser irradiance.

The use of x rays to measure the density of shocked materials was first performed by Johnson and co-workers in the early 1970s.[4] They shocked LiF to several hundred kilobars using conventional explosive

techniques,[5,6] and diffracted a 40-ns to 50-ns pulse of x rays[7] off the shocked material. To our knowledge, however, the work presented here, with a five-hundred-fold improvement in temporal resolution, is the first of a similar nature to be presented since then, and the first time that the launch region has been studied in detail.

The experiment was performed on the JANUS research laser system at the Lawrence Livermore National Laboratory (LLNL). The experimental setup is shown in schematic form in Fig. 29.13. The shocked targets consisted of 250-μm-thick (111) silicon wafers 5 cm in diameter, the surface of which had been coated first with 1000 Å of aluminum and then with 25 μm of parylene (CH). The motivation for such a target design is explained below. Half of the target was irradiated in a vacuum by a 1 ± 0.05-ns pulse of 1.06-μm laser light, at an irradiance varying from 0.8 J cm^{-2} to 8 J cm^{-2} with an on-target beam diameter of 3.9 cm. A beam block prevented irradiation of the other half of the target; diffraction from this unshocked region gave us a reference point from which to measure the changes in Bragg angle. After the shock had been launched in the silicon crystal, a second laser beam containing ~ 10 J of 0.53-μm light in 100 ps, which was synchronous with known and variable delay with respect to the shock-launching beam, was focused to a ~ 40-μm-diameter spot on a second, calcium-containing target. The ionized He-like calcium x-ray lines thus produced[8] were Bragg diffracted off the silicon and recorded on Kodak DEF x-ray film. The reduction in x-ray intensity due to passage through the 25-μm plastic overcoat is estimated to be $\sim 35\%$, with a further $\sim 4\%$ reduction due to passage through the aluminum. A single laser shot provided recordable x-ray levels; a series of shots was taken to obtain data at different irradiances and delay times.

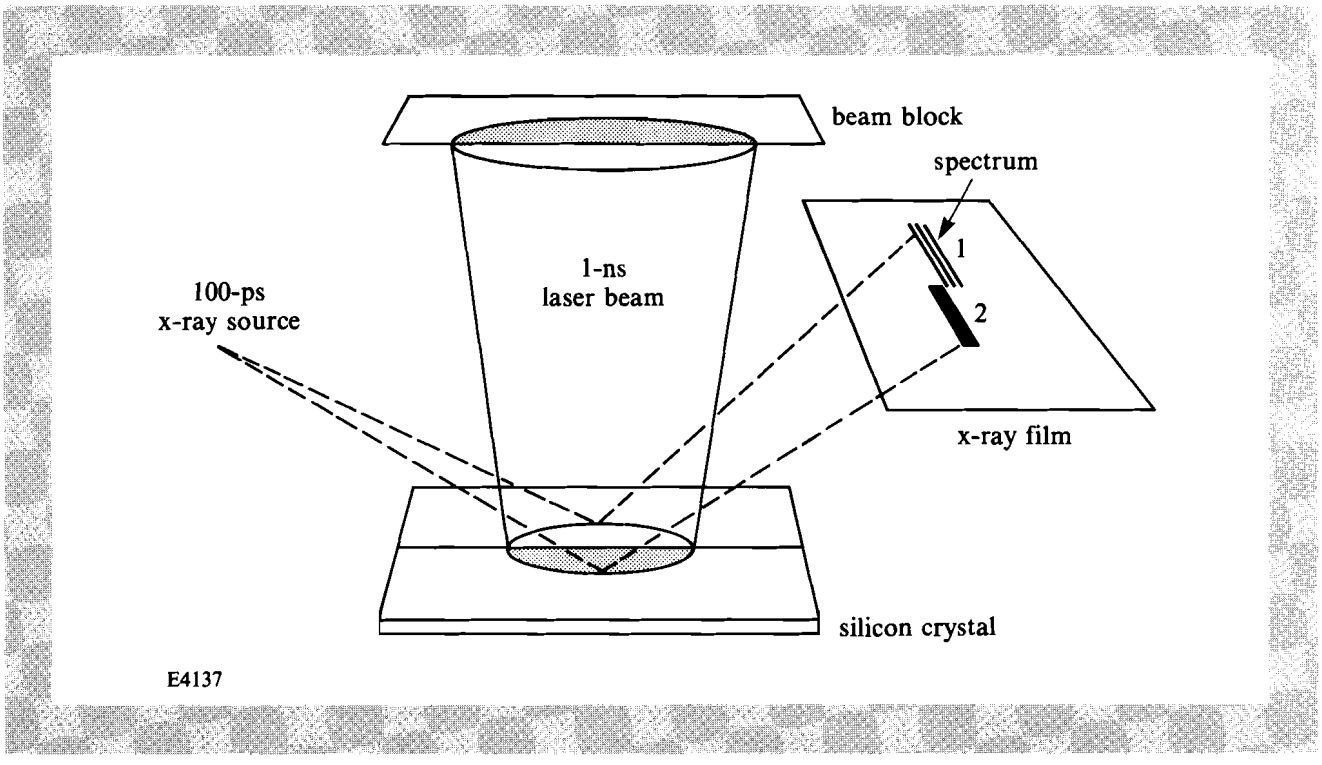

Fig. 29.13
The experimental setup showing schematically the x-ray diffraction from the unshocked (1) and shocked (2) crystal.

Previous experiments at irradiances similar to those used here have shown that uncoated silicon is simply heated by the laser light rather than shocked,[9] due to the several-millimeter absorption length of 1.06-μm light in silicon at room temperature. The aluminum coating was therefore applied to act as an abrupt absorber to the incident radiation. This effectively prevented the penetration of the laser light into the silicon, and instead produced an aluminum plasma that in turn generates a pressure pulse for driving the shock into the material. Overcoating the aluminum with plastic transparent to 1.06-μm light causes the expanding aluminum plasma to be inertially confined between silicon and plastic, which in turn increases the strength of the shock launched into the silicon. Such overcoating techniques have previously been used to enhance shock pressures in the tens-of-kilobar range.[10]

A set of typical diffraction patterns is shown in Fig. 29.14. The three lines in the unshocked region are the resonance line (3.177 Å), the intercombination line (3.193 Å), and the unresolved j, k dielectronic satellites (3.21 Å) of He-like calcium.[8] In the shocked region of the crystal, the lattice spacing d is reduced, increasing the diffraction angle θ in accordance with a differentiation of Bragg's law:

$$\Delta(2d)/2d = -\cot\theta\,\Delta\theta.$$

This effect can clearly be seen in Fig. 29.14. A simple measurement of the maximum angular shift thus gives us a direct measurement of the peak density, and knowledge of the distribution of angular shifts yields information on the distribution of lattice spacings within the probed region.

The probe depth of the x rays in such highly strained crystals is determined by the photoelectric absorption coefficient rather than the extinction length. This is because x rays incident at a particular angle only diffract off that particular region of the crystal at which the lattice spacing is such that the Bragg condition is satisfied; the rest of the crystal up to that point (with slightly different lattice spacings) simply acts as an x-ray filter. A Beer's law attenuation factor of $1/e$ for the He-like calcium lines in silicon corresponds to an x-ray path length of 8.5 μm, or a depth of 4.3 μm below the surface at the Bragg angle. Taking further account of the signal dynamic range, we estimate a probe depth of 4 μm to 5 μm below the surface.

Diffraction measurements such as those shown in Fig. 29.14 were made for a variety of levels of irradiance and delay times. We define the laser beam delay as the interval between the arrival, at chamber center, of the peak of the long (shock-producing) pulse followed by the peak of the short (x-ray-producing) pulse. The x-ray probe delay was 0.09 ns greater than the delay between laser beams, due to the setup geometry and time-of-flight considerations. It can be seen from Fig. 29.14 that at 0.0-ns delay we still observe diffraction at the original Bragg angle as well as diffraction over a range of angles, corresponding to a range of lattice spacings up to a peak compression of 3.35%. The obvious physical explanation for this is that, at this

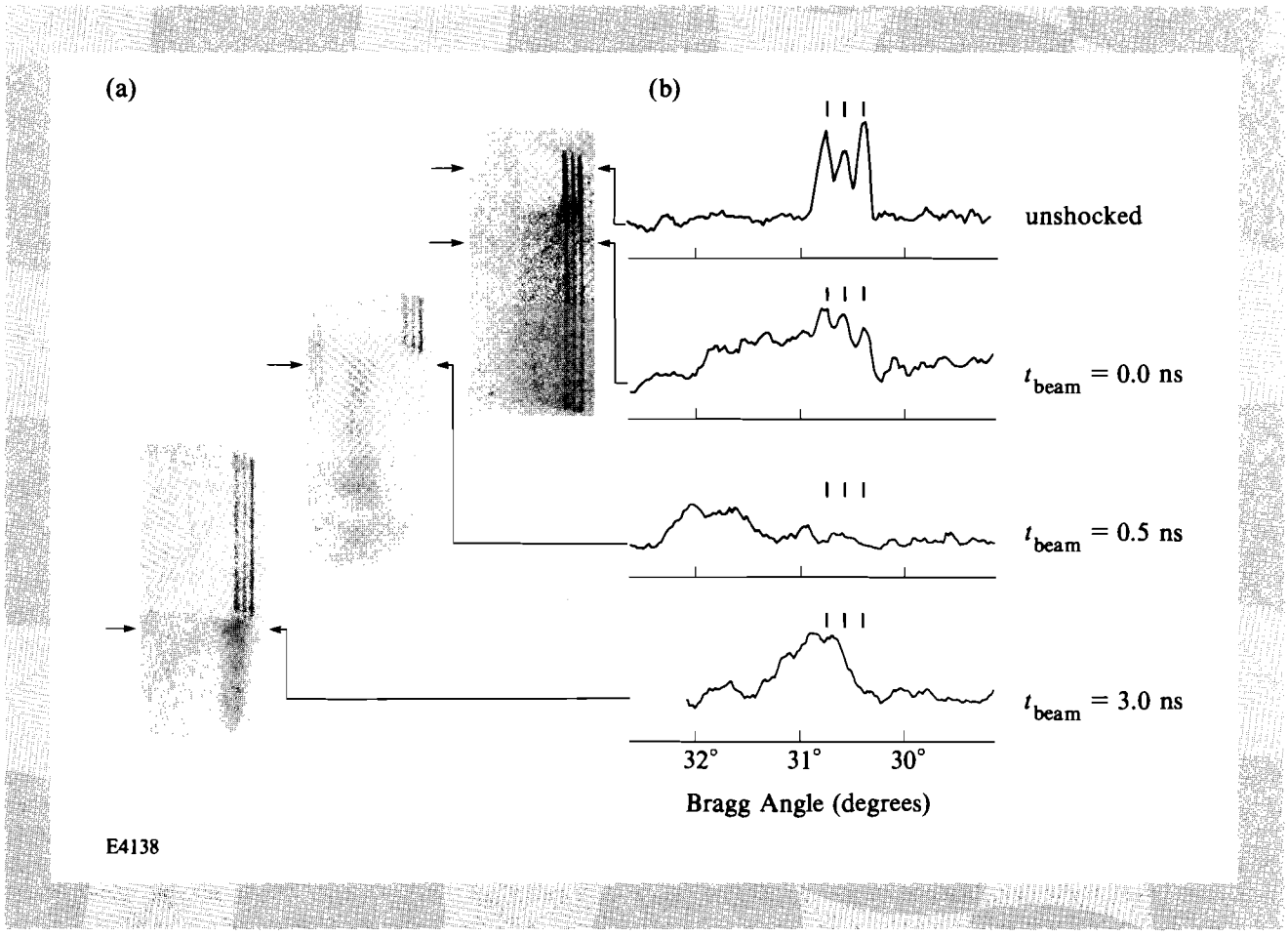

Fig. 29.14
Diffraction results.
(a) X-ray line spectra diffracted from silicon shocked at an incident-energy density of 4 ± 0.3 J cm^{-2} (an irradiance of 4×10^9 W cm^{-2}) are shown adjacent to reference lines simultaneously diffracted by the unstrained silicon lattice, from a series of beam delays. Each photograph represents a separate shot and beam delay.
(b) Densitometer scans, taken at indicated locations through the spectra in (a), are shown for a typical unshocked spectrum, and shocked spectra at 0.0-ns, 0.5-ns, and 3.0-ns beam delays.

early time, the shock has not yet penetrated past the maximum probe depth, and we are probing through the shock front into the as-yet-unshocked region. For all data collected after this delay time, when the shock has proceeded further into the material, we no longer observe diffraction from the unperturbed crystal.

In Fig. 29.15 we show the peak change in interatomic spacing as a function of time for those shots where the average energy density of the shock-producing laser pulse was 4 ± 0.3 J cm^{-2} on target (i.e., an average irradiance of 4×10^9 W cm^{-2}). The accuracy of the laser timing may include a constant systematic error estimated to be no more than ± 200 ps; random timing fluctuations were evidently of lesser magnitude. The error bar on the density measurement results primarily from a consideration of observed effects of laser nonuniformities on the maximum Bragg diffraction angle. [These

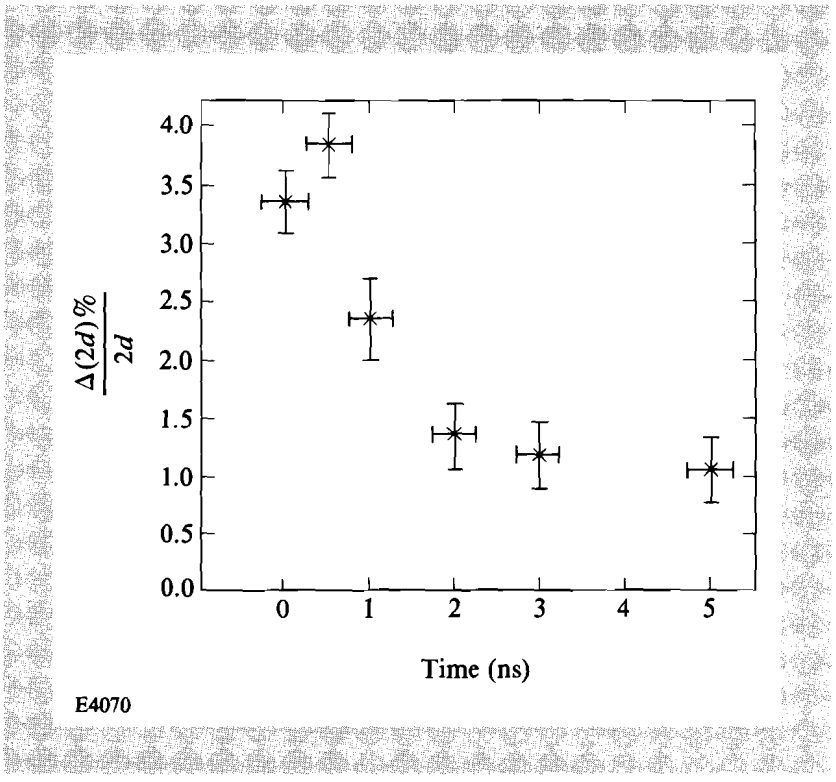

Fig. 29.15
The measured peak change in interatomic spacing as a function of time for those laser shots with an energy density of 4 ± 0.3 J cm^{-2}.

effects can be seen in Fig. 29.14(a) as a variation in angular shift in the diffracted radiation.] Other effects, such as intrinsic x-ray line width, crystal rocking curve breadth, and x-ray source broadening, are of considerably lesser importance. A maximum change of the lattice spacing of 3.85% was observed at this energy density, and the data are consistent with a pressure pulse with a FWHM of 1 ns. It can be seen that the rise time of the shock compression is similar to that of the laser pulse. However, after peak compression has been reached, the density falls off with a far longer decay time than that of the laser. Indeed, even 5 ns after the peak of the shock-producing pulse, the crystal is still compressed by $\sim 1\%$. At no time did we observe the front-surface density to fall below that of solid. Such inhibition of the rarefaction wave has previously been observed by other diagnostic methods[11] (using similar tamped targets), and is due to the tamping effect of the plastic.

The Hugoniot elastic limit (HEL) has been reported to occur in (111) silicon at a compression of 2.6%,[12,13] corresponding to a pressure of about 54 kbar. Applying the stress-volume curve of Gust and Royce[12] to the observed 3.85% compression, we estimate a peak stress of 67 kbar at an energy density of 4 J cm^{-2}. However, in comparing these results to Hugoniot measurements, it should be borne in mind that we are probing the shock-launching phase, rather than merely observing the arrival of an already steepened shock front. Furthermore, elastic response may extend above the HEL on a transient basis.[14,15]

Figure 29.16 shows the experimentally measured peak compressions as a function of irradiance for various probe delay times. The rapid

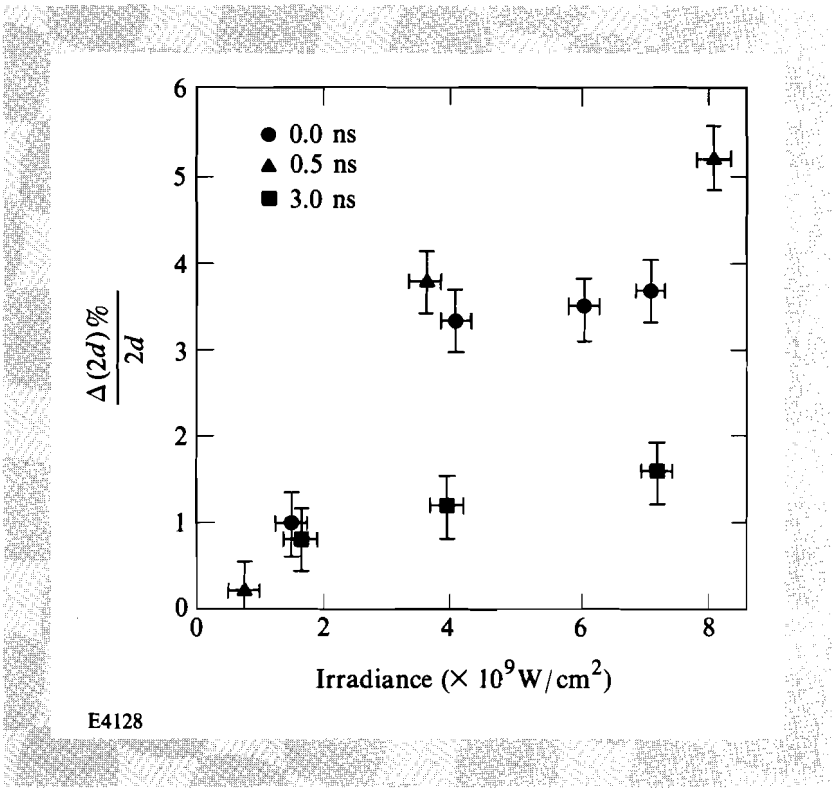

Fig. 29.16
The peak change in interatomic spacing as a function of irradiance for delay times indicated. The HEL is at 2.6% compression.

falloff in compression at low irradiances is due to the increased importance of thermal conduction into the silicon at lower irradiances,[11] as well as an increase in the fraction of laser energy expended in the latent heat of vaporization of the aluminum.

The technique of pulsed x-ray diffraction from laser-shocked materials opens up several new avenues for the study of the transient response of crystal lattices. For instance, while we have shown here that it is possible to measure the density on the front surface of a shocked crystal, the technique can obviously also be applied to the rear surface. Because the x rays can probe through the crystal, we can in principle observe a shock wave before, during, and after arrival at a free surface, making density measurements at any stage for any sample thick enough to diffract. The temporal resolution afforded by this technique, coupled with its ability to probe crystal structure, may allow us to time-resolve pressure-induced phase transitions, as well as study possible transient effects in crystals compressed beyond the HEL.[14,15] Furthermore, a detailed study of the x-ray reflectivity as a function of angle may yield density-depth information, using methods similar to those developed for studying laser-annealed crystals.[16,17]

Significant advances have recently been achieved in the uniformity with which pulsed lasers can irradiate a target,[18] which we anticipate may lead to a major improvement in the uniformity of laser-generated shocks. Such improvement would enhance the precision of x-ray diffraction and a wide range of other measurements involving laser-generated shocks. Also of particular importance to x-ray probing is the advent, within the next few years, of laser pulses as short as 1 ps

capable of producing x rays with the intensities necessary for single-shot recording.[19,20]

In conclusion, we have directly observed the temporal history of density change within a laser-shocked crystal by short-pulse x-ray diffraction. We have observed diffraction from material both in front of and behind the developing shock front at early stages during the laser drive pulse. We have followed the lattice compression to values above the HEL, and further observed the onset of rarefaction as the pressure pulse decayed. Crystallinity was preserved throughout this process.

ACKNOWLEDGMENT

This work was supported by the U.S. Department of Energy Office of Inertial Fusion under agreement No. DE-FC08-85DP40200 and by the Laser Fusion Feasibility Project at the Laboratory for Laser Energetics, which has the following sponsors: Empire State Electric Energy Research Corporation, General Electric Company, New York State Energy Research and Development Authority, Ontario Hydro, and the University of Rochester. Such support does not imply endorsement of the content by any of the above parties.

Research was performed in collaboration with the U.S. Naval Research Laboratory and Los Alamos National Laboratory. The author acknowledges the assistance of the staff of the JANUS research laser system at the Lawrence Livermore National Laboratory.

REFERENCES

1. L. C. Yang, *J. Appl. Phys.* **45**, 2601 (1974).
2. A. N. Pirri, *Phys. Fluids* **20**, 221 (1977).
3. B. P. Fairand, B. A. Wilcox, W. J. Gallagher, and D. N. Williams, *J. Appl. Phys.* **43**, 3893 (1972).
4. Q. Johnson, A. Mitchell, R. N. Keeler, and L. Evans, *Phys. Rev. Lett.* **25**, 1099 (1970).
5. Q. Johnson, A. Mitchell, and L. Evans, *Nature* **231**, 310 (1971).
6. Q. Johnson, A. C. Mitchell, and L. Evans, *Appl. Phys. Lett.* **21**, 29 (1972).
7. Q. Johnson and A. C. Mitchell, *Phys. Rev. Lett.* **29**, 1369 (1972).
8. U. Feldman, G. A. Doschek, D. J. Nagel, R. D. Cowan, and R. R. Whitlock, *Astrophys. J.* **192**, 213 (1974).
9. J. G. Lunney, P. J. Dobson, J. D. Hares, S. D. Tabatabaei, and R. W. Eason, *Opt. Commun.* **58**, 269 (1986).
10. N. C. Anderholm, *Appl. Phys. Lett.* **16**, 113 (1970).
11. B. P. Fairand and A. H. Clauer, *J. Appl. Phys.* **50**, 1497 (1979).
12. W. H. Gust and E. B. Royce, *J. Appl. Phys.* **42**, 1897 (1971).
13. T. Goto, T. Sato, and Y. Syono, *Jpn. J. Appl. Phys.* **21**, L369 (1982).
14. J. R. Asay, G. R. Fowles, G. E. Duvall, M. H. Miles, and R. F. Tender, *J. Appl. Phys.* **43**, 2132 (1972).
15. Y. M. Gupta, G. E. Duvall, and G. R. Fowles, *J. Appl. Phys.* **46**, 532 (1975).